ICAS 2021 SHANGHAI
International Council of the Aeronautical Sciences
32nd Congress of the International Council of the Aeronautical Sciences
September 6-10, 2021
Pudong Shangri-La, Shanghai, China

NUMERICAL SIMULATION AND EXPERIMENTAL INVESTIGATION ON FLUTTER AND NON-SYNCHRONOUS VIBRATION

Liu Yixiong[1,*], Mo Da[1], Du Qing[1], Chen Yuzhi[1], Wang Meng[1]

[1,*]AECC Shenyang Engine Research Institute, 110015, China

Abstract

This paper aims at exploring the primary characteristics of fan blade flutter and compressor non-synchronous vibration (NSV) phenomenon by experimental investigation and numerical simulation. The multi-physical field synchronized measurement was implemented to monitor the dynamic stress, pressure fluctuation, blade tip vibration at the same time. The features of fan blade flutter at 0.75 corrected speed and compressor NSV at idle condition were achieved and compared. Afterwards, the corresponding aero-work and aerodynamic damping were obtained using the phase-shifted energy approach. Results show both flutter and NSV occupied locked phase and frequency, non-integer engine order excitation and nodal vibration features. However, the flutter demonstrated a forward wave vibration with 4 nodal diameter whereas NSV showed a backward wave vibration with 13 nodal diameter. Furthermore, flutter was found near the surge line with sharply increased stress to 187Mpa within seconds while the NSV would maintain a large stress level near the idle working line. The total aero-work for flutter was positive while it was negative for NSV, which implies that the aerodynamic damping was not enough to curb the vibration during flutter. The numerical simulation is consistent with experimental results.

Keywords: Flow-induced vibration; Aerodynamic damping; Dynamic stress; Frequency; Nodal diameter

1. Introduction

Flow-induced blade self-excited vibrations, including flutter and NSV [1], have drawn the attention of both aerodynamic researchers and structural researchers over the past few decades. Unlike forced response, no direct excitations related to upstream and downstream vanes or inlet distortion in the stationary frame were observed, indicating that the phenomena cannot be predicted simply by the Campbell diagram[1-2]. Studies focus on empirical methods at earlier times, hoping to achieve a similarity criterion that could be applied to predict flutter, but with low accuracy[3-4]. The primary reason is that flutter is a fluid-structure interaction (FSI) issue that has a mutual relationship between blade vibrations and unsteady aerodynamic pressure. Consequently, it is hard to obtain a deeper insight into the mechanism only by some design parameters. In order to explore the mechanism of flutter and perform a precise prediction of the aero-elastic stability of blade, eigenvalue methods and energy methods as well as coupled methods were developed[5], which laid the foundation of modern computational fluid dynamic methods.

Eigenvalue method is actually to solve the motion differential equation with the excitation force converted to the unsteady aerodynamic force. It provides a deeper insight into understanding the vibration frequency, mode and phase. Bendiksen and Friedmann[6] used the eigenvalue method to deal with the cascade flutter and found it effective when considering bending-torsion coupling blade flutter. Fu [2] [7] made a thorough introduction of eigenvalue method and studied the aero-elastic stability of an axial compressor blade. The results were in good agreement with the experimental results. It is well-established that the eigenvalue method combining the influence coefficient[8] method has become the most commonly accepted approaches to assess the mistuned effects on the aero-elastic stability of rotor blades.

Carta[9] first came up with a method, which Bendisk[10]called energy method for flutter prediction. The main principle is to judge whether the absorbed energy from the nearby flow field is consumed

by the blade vibration system. Correspondingly, aerodynamic damping is often regarded as the criteria to determine aero-elatic stability since it is dimensionless. Considering the energy method is capable of interacting with various aerodynamic models, such as the two-dimensional strip theory and the three-dimensional model, it has been widely accepted and developed by numerous researchers. Snyder and Commerford[11] investigated the effects of Mach number, reduced frequencies, incidence angles and interblade phase angles(IBPA) on supersonic un-stalled flutter by utilizing the energy method. The results coped well with experiments even if the aerodynamic model was based on plate cascade theory. Erdos[12] first introduced the direct store method to record the data on the periodic boundaries considering phase difference. Nevertheless, it required tremendous computing resources and cannot be unaccepted in solving three-dimensional unsteady aerodynamics. He[13] proposed the Fourier transform method by applying the Fourier series decomposition in the time-domain. The variable information can be analyzed at any time step by only memorizing certain Fourier coefficients. Then He and Denton[14] employed the method into three-dimensional unsteady flow calculation. Since the whole passage model calculation was time-consuming and unacceptable in practice, the Fourier-transform method witnessed promising prospects in flutter predication.

The coupled method can be divided into two categories: iterative methods and full methods. Iterative methods have to solve the aerodynamic model and structural model respectively and exchange information at each step until reaching the steady oscillation. Full methods combine the two models in the same equation groups and solve them at each step. As the coupled methods are too complex and need a large amount of calculation, there is still a long way to go before they are applicable in engineering.

Numerous experiments were conducted throughout the years, together with theoretical model investigations and numerical simulations, providing a comprehensive understanding of the flutter mechanism. Sanders[15] performed a systematical test of blade flutter with pressure transduces mounted on the 90% span to measure aerodynamic loading and strain gages mounted to measure the vibratory frequency. Some typical features of stall flutter were obtained, though not first observed, such as phase and frequency locked, incipient and deep flutter regions, non-synchronous, forward wave. But there were some phenomena not mentioned, such as the frequency patterns and the effects of upstream vanes. M. Baumgartner[16] explained the frequency patterns through theoretical formulation and confirmed that in a high-pressure compressor experiment. One is that there exist two side frequencies near the blade passing frequency (BPF) [17]. Another is that source frequency could excite pressure waves with multiple nodal diameters, which was mentioned by other experiments[18-21]. As for the parameters influencing stall flutter and NSV, most attention has been focused on incidence angles, IBPA and inlet Mach numbers[22-24]. Huang[25] and Sun[26] explored the possibilities to prevent flutter by open or close the upstream stators but without experimental supports.

Both experiments and numerical calculation were carried out in this paper to investigate the frequency patterns and the dynamic pressure fluctuation as well as the aerodynamic damping. The synchronized test system of multi-physical field parameters was utilized to measure critical parameters, providing convincing evidence to examine the driving mechanism for aerodynamic instability[27]. High response pressure transducers, strain gauges and optical fibre sensors were installed to capture the features when the blade was encountering flutters and NSV. The phase-shifted energy method adopted and developed from [2] and [28] was also implemented to predict the aerodynamic stability of the blade, aiming at obtaining the nodal diameters with negative aerodynamic damping and the influences of the upstream vane, which could tie up with the tested results.

2. Experimental Investigation

2.1 Cases study

There are two cases investigated regarding to the flutter and NSV characteristics. A second stage fan blade with 38 blades was studied to conduct the flutter experiment and numerical simulation. A first stage compressor blade with 38 blades was established for the NSV investigation. The materials for the fan blade and the compressor blade are both Titanium alloy. Furthermore, the

flutter was predicted and tested at 0.75 corrected speed by pushing the operating point from working line to surge line. On the contrary, the NSV was tested and simulated at idle condition near the working line. By observing the altering of the dynamic stress, pressure fluctuation and blade tip deformation, the characteristics of flutter and NSV were obtained.

2.2 Measurement Approaches

As has been revealed by Sanders[15] and Kielb[1], both flutter and NSV are caused by the non-integer engine order excitation. Besides, the pressure fluctuation frequency is related to the vibration frequency. Therefore, vibration and dynamic pressure characteristics would be monitored to distinguish the two type of flow-induced vibrations. In this scenario, the strain gauges, high response Kulite pressure transducers and optical fibre sensors were implemented to perform the experimental investigation. There are 38 blades for the investigated fan and compressor respectively, which were divided into two opposite sections along the circumferential direction. As the measurement strategies of the fan and the compressor are almost the same, the fan blade measurement was described in detail. As presented in Figure 1 a), two strain gauges were mounted in one blade to figure out the first bending and torsion mode, which are easily prone to aero-elastic instability. In order to identify the travelling wave and the nodal diameter, six adjacent blades were employed with two strain gauges mounted, as shown in Figure 1 c). The oppositely distributed two sections would also reveal the flutter vibratory characteristics and incorporate the weight balance consideration.

Eight high response Kulite pressure transducers were also mounted on four blades surface located at the 90% span to observe the pressure fluctuation when encountering aerodynamic instability, as depicted in Figure 1 b). To be specific, two transducers were located at the 1/5 and 4/5 chord on the suction side of one blade while the other two were mounted on the 2/5 and 3/5 chord on the pressure side of another blade. It should be noted that the two blades were in one cascade to closely observe the dynamic pressure fluctuation, as shown in Figure 2. Similarly, there are eight transducers mounted on the blade surface, as shown in Figure 1 c). Meanwhile, the optical fibre sensors were utilized to trace the leading and trailing blade tip vibration amplitude with three sensors installed along the circumferential direction for each axial location, as depicted in Figure 3.

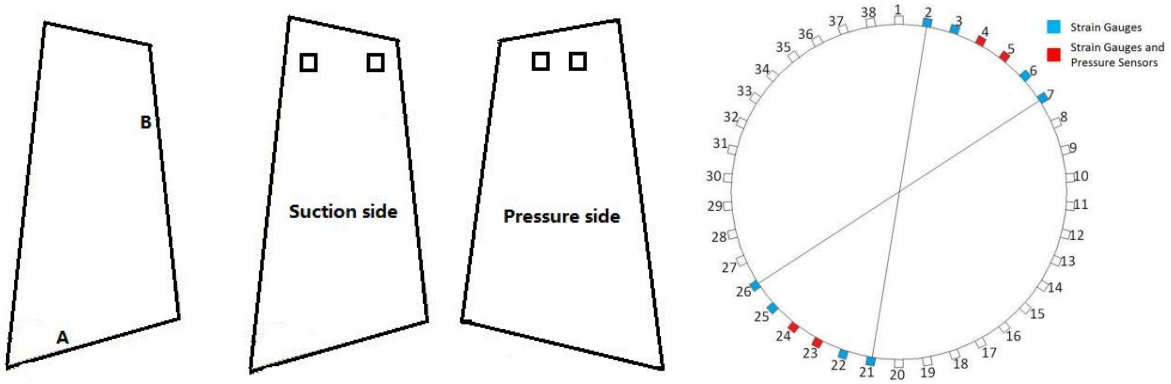

a) Strain gauges b) Pressure transducers on blade surface c) Circumferential distribution

Figure 1 – Strain gauges locations

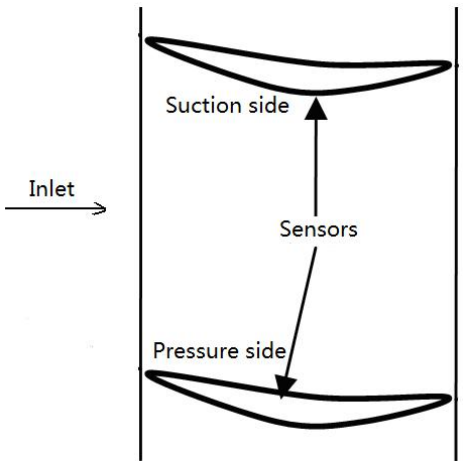

Figure 2 – Pressure transducers distribution in one cascade

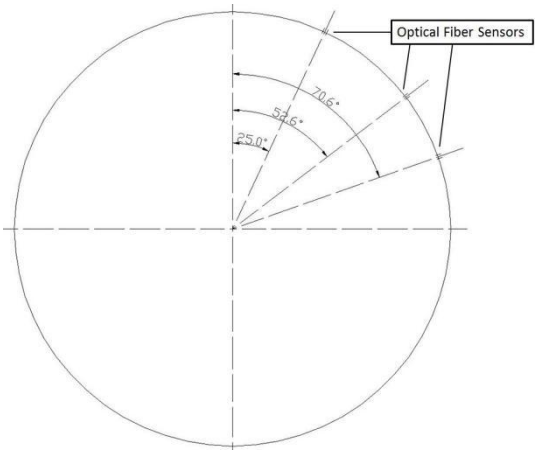

Figure 3 – Optical fibre sensor distribution

It is well established that flutter and NSV duration are relatively short, indicating that the vibration stress and dynamic pressure should be measured in the same time domain. Besides, a deeper insight into the fluid-solid coupling mechanism would be obtained if the time sequence of the vibration and the pressure is retained. In this scenario, the multi-physical filed steady/dynamic signal synchronization experiment was implemented to collect the parameters, as shown in Figure 4. The acquisition system deploys 64 channels composing of 42 channels for noise or dynamic pressure and 22 channels for strain gauges. The sampling frequency reaches 200 kHz while the data could be processed within 80 kHz band width[27]. A time-based and speed-based calibration was carried out at the beginning of the test to synchronize all the signals.

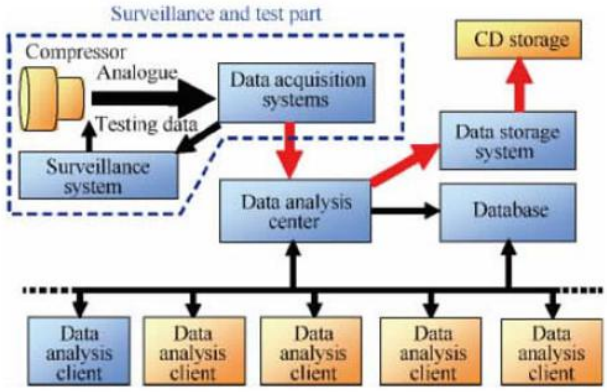

Figure 4 – Scheme of the multi-physical field steady/dynamical signal synchronization[27]

2.3 Results of flutter

2.3.1 Vibration characteristics

For the fan blade case, the aero-elastic stability test was performed from 0.7-0.85 corrected speed by pushing the operating point close to the surge line at a fixed corrected speed. The experimental results of 0.75 corrected speed were thoroughly described to demonstrate the flutter vibration features. As can be seen in Figure 5, there existed several low responses with various frequencies at the working condition. However, as the operating point moves towards the surge point along the constant speed line, the frequencies of all the strain gauges were tuned to one specific frequency, which is the flutter frequency. Closer inspection on the figure shows that the flutter frequency was not far away from the first bending frequency, indicating the fan blade was encountering the first bending mode flutter. Furthermore, the vibration stress remained extremely low and then soared to 187MPa within 5s, revealing a rapid and divergent trend. Another observation is that the vibration phase was locked at the flutter condition with all the signals demonstrating a sine curve, as depicted in Figure 6.

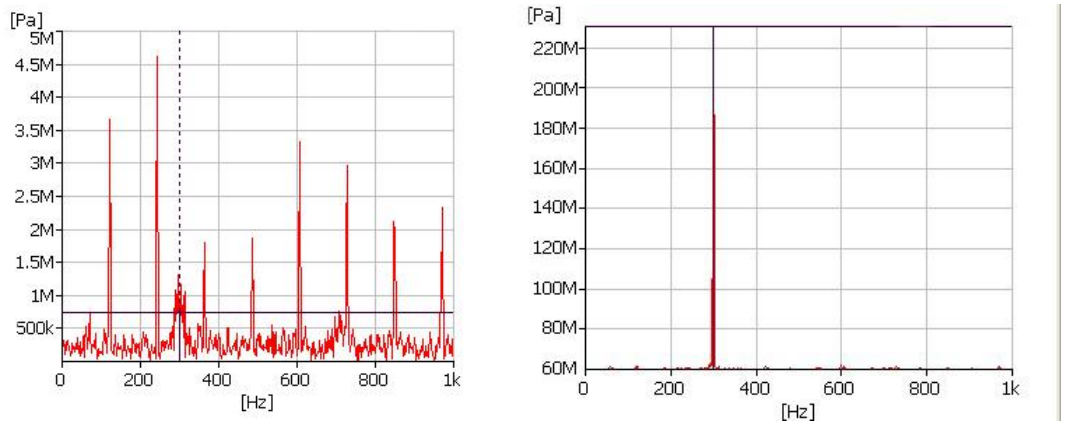

a) Steady state b) Flutter state

Figure 5 – Flutter frequency locked near the first bending frequency at 0.75 corrected speed

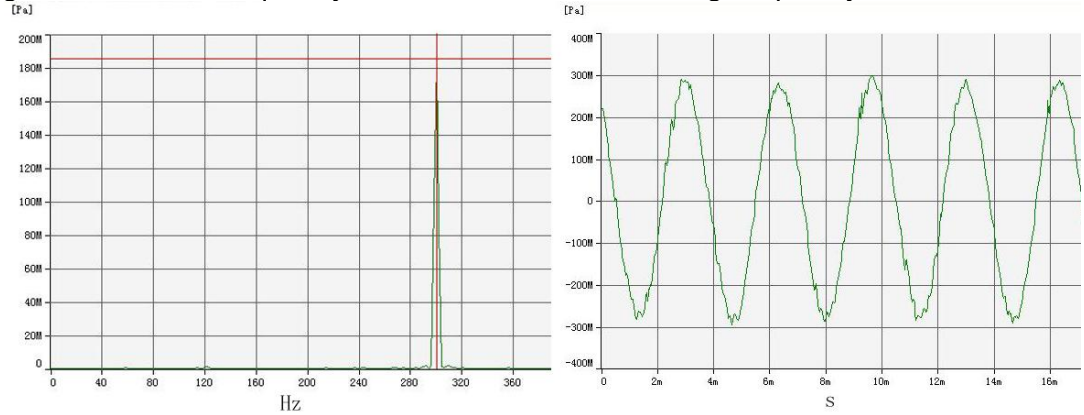

Figure 6 – Phase-locked at 0.75 corrected speed during flutter

Another critical feature of flutter is that the excitation is not the engine orders (EO), as can be seen in Figure 7. The waterfall plot implies that the high stress is not linear to the corrected speed but locked at the flutter frequency with 2.47EO excitation. The vibration response of the two sections indicates that all the blades were suffering from the fluid-solid interaction effects during flutter, as shown in Figure 8. Furthermore, the optical fibre sensor results showed that the blades tip amplitude was in nodal form resulting from the coupling of pressure waves and the vibratory waves. The estimated nodal diameter was about four with the maximum amplitude reaching 7.5mm, as depicted in Figure 9.

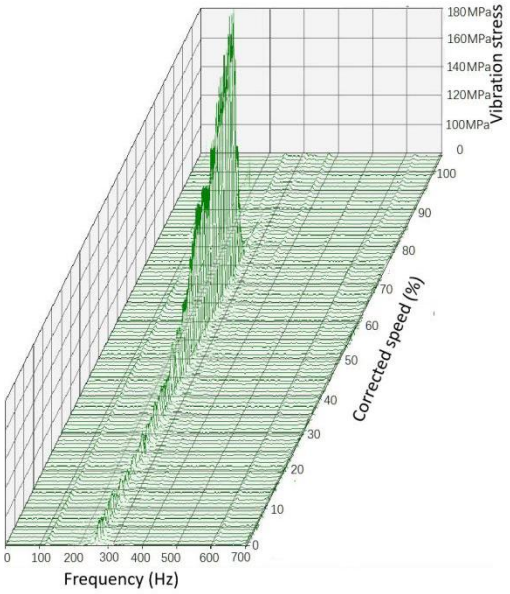

Figure 7 – Non-integer engine order excitation

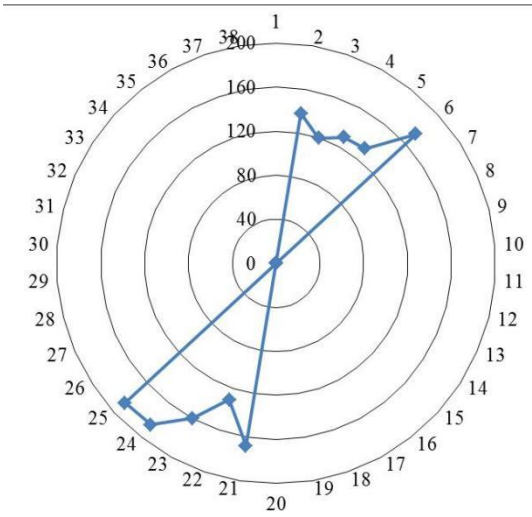

Figure 8 – Vibration stress in the opposite sections

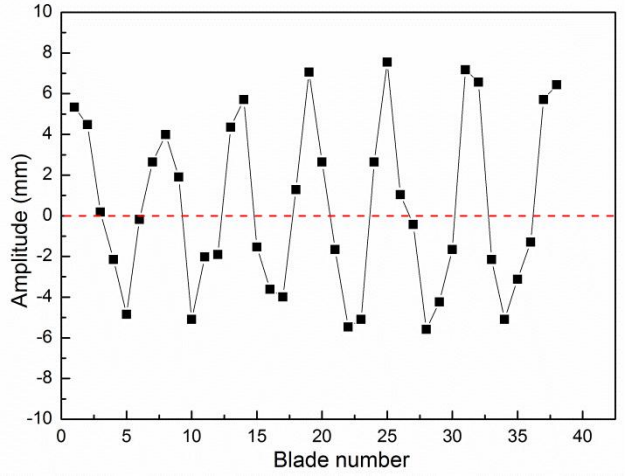

Figure 9 – Blade tip vibration amplitude during flutter at 0.75 corrected speed

2.3.2 Dynamic pressure characteristics

The dynamic pressure signal was analyzed using the FFT approach with the high response frequencies depicted in Figure 10. The top response approached 3900 Pa at 788 Hz, which is the characteristic frequency. Meanwhile, the 3030Hz and 4610 Hz were the blade passing frequency (BPF) of the first stage and second stage blades ranking the second-highest response. The 3820Hz was the so-called left side frequency, which equals the second stage BPF minus the characteristic frequency. Further analysis on the relationship between the vibration frequency and dynamic pressure characteristic frequency was listed in (1). There existed a connection between the frequencies in the rotatory and stationary frame. It occurs that the pressure characteristic frequency in the stationary frame equals the vibration frequency in the rotatory frame plus the four times the fundamental frequency. The indicated vibration form is a four nodal diameter forward wave vibration with the locked vibration frequency at the first bending mode. It reveals that the investigated fan blade has encountered a typical subsonic flutter at low corrected speed. Furthermore, the dynamic pressure first showed an upward trend and approached the peak during flutter whereas the vibration stress demonstrated a sudden increase only when the operating point moved close to the flutter point, as depicted in Figure 11. This phenomenon implies that flutter is a process of energy accumulation induced by flow instability.

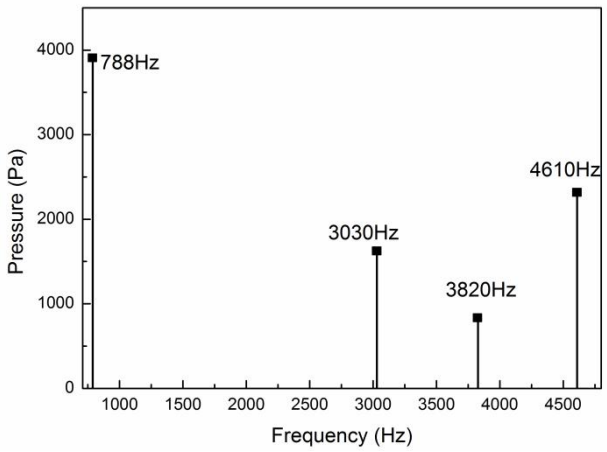

Figure 10 – Dynamic pressure frequencies

$$F_S = F_R + mF_F \tag{1}$$

Where：

F_F is the fundamental frequency（Hz）

m is the nodal diameter

F_S is the dynamic pressure characteristic frequency in the stationary frame（Hz）

F_R is the vibration frequency in the rotatory frame（Hz）

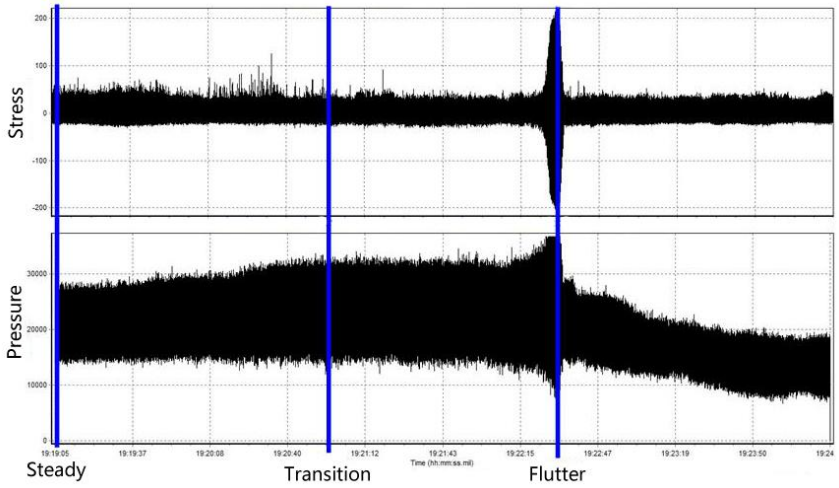

Figure 11 ─ Time sequence for the dynamic pressure and vibration stress

2.4 Results of NSV

Similar to the fan blade flutter test, the compressor NSV test was performed in the same test rig with the previously mentioned measurement devices. Besides, the distributions of the strain gauges and sensors were almost the same. It should be noted that the compressor NSV was mainly discovered in idle condition. Obviously, the compressor NSV also showed frequency and phase locking phenomenon at the first bending mode, which would not be listed in detail. The excitation was non-synchronous engine order reaching approximate 7.5. Meanwhile, the blade tip amplitude measuring by the optical fibre sensors revealed that the NSV would also generate lobed shape vibration, as shown in Figure 12. The maximum amplitude approached 3.0mm during NSV, which was unacceptable for the compressor blade.

However, there existed several differences between the flutter and NSV. Firstly, the NSV revealed a backward wave trend using (1) with the nodal diameter 13, which was a fundamental feature differing from flutter. The corresponding vibration frequency and pressure characteristic frequency were 600Hz and 1500Hz respectively, as shown in Figure 13. Secondly, the corrected speed for flutter and NSV differed with flutter occurring at 75% corrected speed whereas the NSV bursting at idle condition. To be specific, flutter was observed when near the surge line but the NSV initiated not far away from the working line. The NSV stress would first go up and then lowered down when the operating point moved towards the surge line. More importantly, the NSV could maintain a stable stress level peaking at 150MPa while the flutter stress could hardly converge and outbreak

rapidly, as presented in Figure 14.

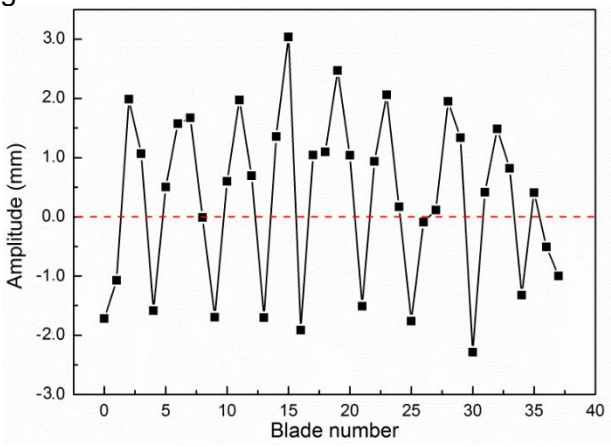

Figure 12 ─ Blade tip vibration amplitude during flutter at idle condition

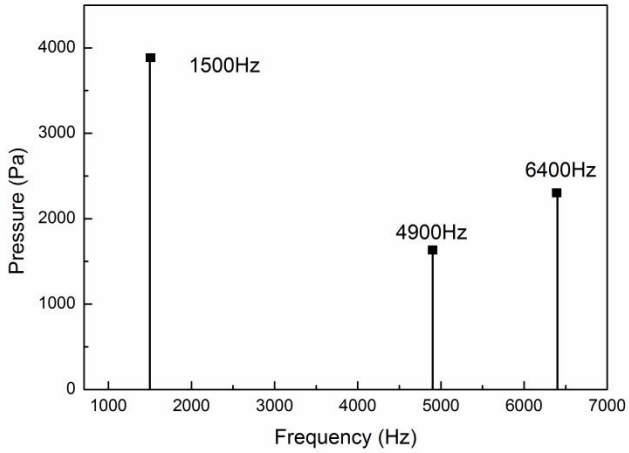

Figure 13 ─ Dynamic pressure frequencies

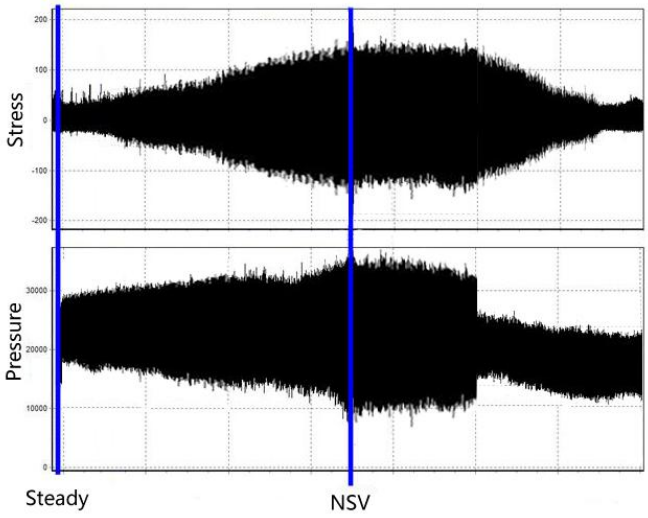

Figure 14 ─ Dynamic pressure frequencies

3. Numerical Simulation

3.1 Phase-shifted energy method

The phase-shifted energy method [2] was implemented to investigate and compare the characteristics of flutter and NSV. It is developed from the energy conservation perspective by calculating the energy obtained from the fluid and the energy consumed for the whole vibration system. A small initial vibration amplitude was assumed to impact the fluid, and then interactions between the fluid and structure were started. The primary assumptions were that the fluid had minor effects on the vibration and the mechanical damping was far lower than the aerodynamic damping. Therefore, the aerodynamic stability of the blade could be obtained by (2). In order to assess the

blade stability with dimensionless data, aerodynamic damping was introduced, as listed in (3). Negative aerodynamic damping represents that the system has consumed the energy and would remain stable.

Furthermore, the interblade phase angle has enabled the implementation of the phase-shifted energy method by using the Fourier series decomposition approach. The variable information at each time step would be attained from the coefficient calculation, as listed in (4). In this scenario, the double-passage fluid model was utilized to accelerate the simulation with implicit solutions.

$$W(\vec{x},t)=\int_0^{0+T_{blade}} P(\vec{x},t)\vec{V}(\vec{x},t)\bullet\vec{n}(\vec{x},t)dt,\forall x\in\partial B \tag{2}$$

$$\xi_i=-\frac{W_{cfd}}{2\pi q_{i0}^2 w_i^2} \tag{3}$$

$$f(t)=\sum_{n=-M}^{M} A_n e^{-i(wnt)} \tag{4}$$

3.2 Flutter prediction

Both the finite element model and fluid model were established to achieve the modal deformation and steady-state performance, as shown in Figure 15 a) and b). The nodes for the two models were 10395, 50200 respectively. The deformation of the first bending mode is depicted in Figure 15 c), indicating that the maximum deflection occurs at the tip of the leading edge. The nodal deformation would be interpolated with the fluid model during the transient analysis. The unsteady analysis was performed using the steady-state results as the initial condition to aid the convergence. Besides, the aerodynamic damping and the total work in an oscillation period were obtained after several iterations.

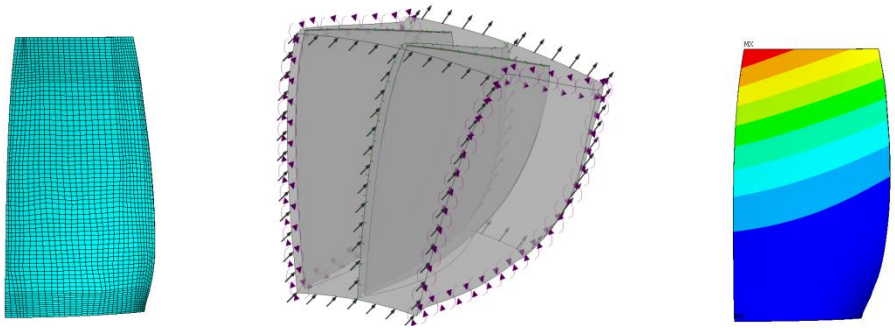

a) Finite element model b) Double-passage fluid model c) First bending mode

Figure 15 ─ Model establishment

The aerodynamic work distribution of the fan blade is presented in Figure 16. It could be seen that the positive work region mainly concentrates on the suction side trailing edge, indicating a severe flow separation in this area. Although the positive work region was relatively small, the total positive work has exceeded the consumed work, meaning that the energy was accumulated in the system and would generate flutter. The calculated aerodynamic damping at 0.75 corrected speed was -1.436E-3, revealing a flutter risk.

Further analysis in Figure 17 shows that the flutter was a forward wave vibration as validated by the experiment. Point 1 and point 2 were located at the blade tip, as depicted in Figure 17 a). The vibration was transferred from point 2 to point 1 with a sin curve, representing a tuned vibration by the flow. Finally, the flutter boundary was predicted at low corrected speed conditions, as presented in Figure 18. Obviously, the working line was close to the predicted flutter boundary as the dashed line implied. Moreover, the calculated boundary was more aggressive than the measured boundary, which was advantageous in a conservative flutter forecast.

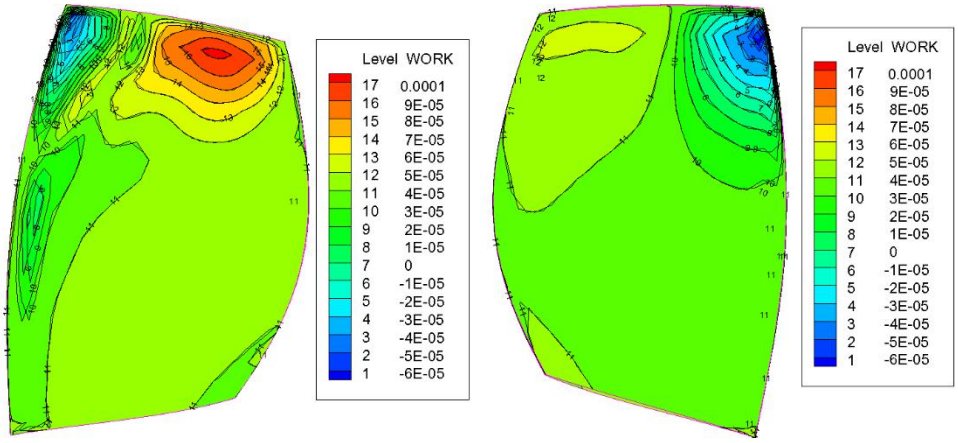

a) Suction side b) Pressure side

Figure 16 ─ Aerodynamic work distribution on the blade surface

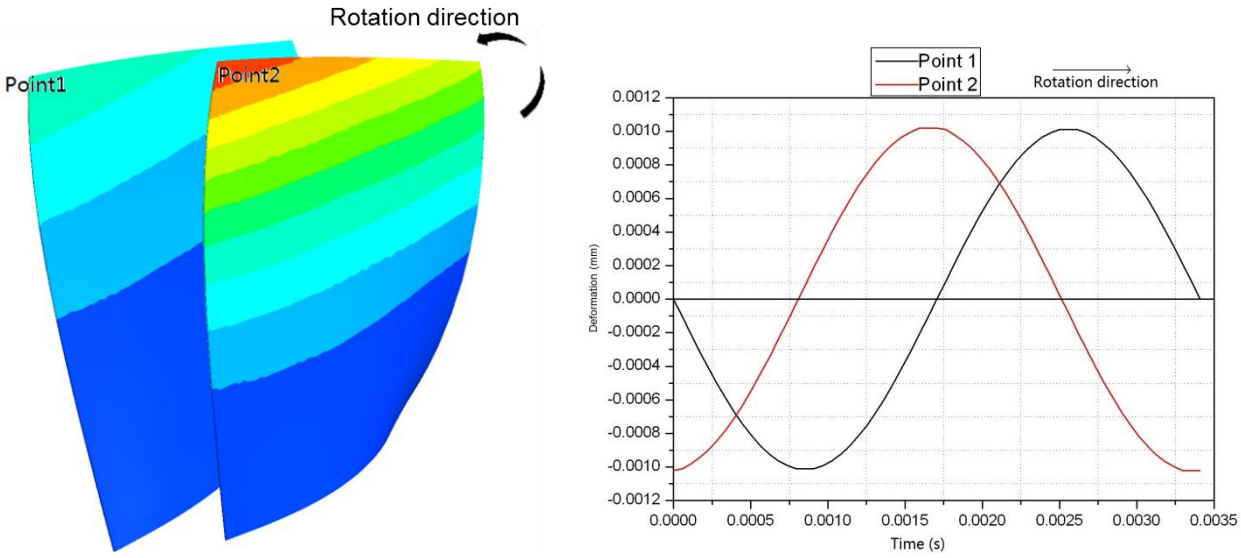

Figure 17 ─ Forward wave vibration

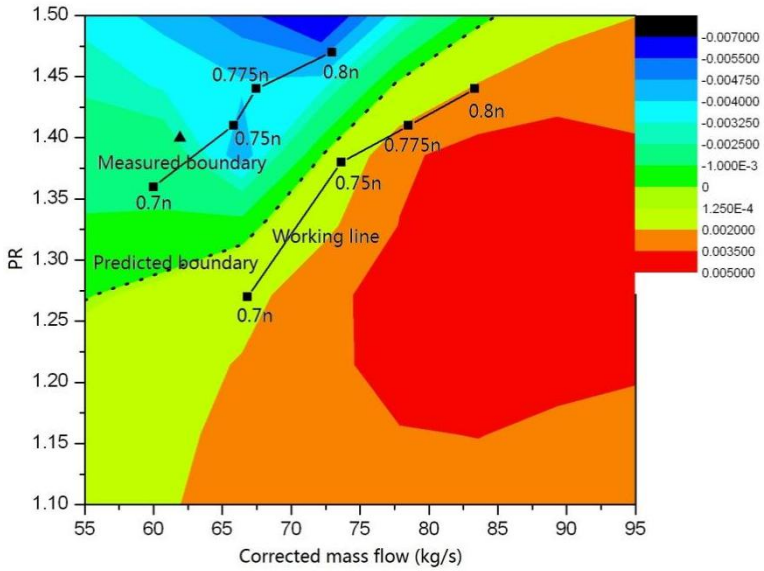

Figure 18 ─ Fan blade flutter boundary prediction

3.3 NSV Prediction

The finite element model and fluid model were built for compressor NSV prediction, as shown in Figure 19 a) and b). The deformation of the first bending mode was similar to the fan blade with the blade tip employed the largest amplitude, as shown in Figure 19 c). Afterwards, the transient

analysis was carried out to simulate the weak coupling of blade and fluid. The aerodynamic work of the compressor was demonstrated in Figure 20. What is interesting is that the positive work region was also found at the suction side trailing edge but with tiny values. The corresponding aerodynamic damping ratio was 5.067E4 which implies a steady state. This characteristic was regarded as the fundamental contrast between flutter and NSV.

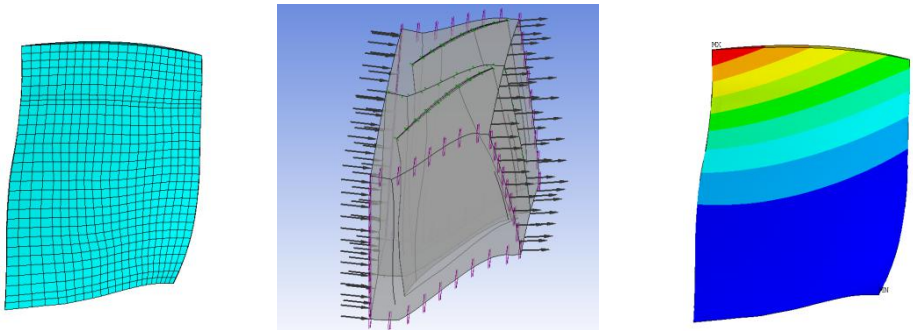

a) Finite element model b) Double-passage fluid model c) First bending mode

Figure 19 ─ Model establishment

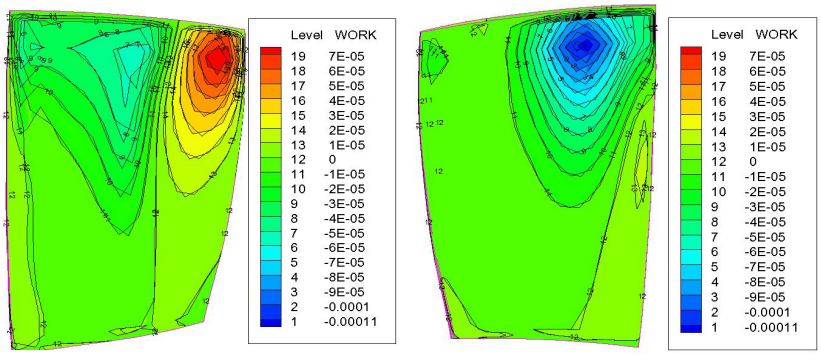

a) Suction side b) Pressure side

Figure 20 ─ Aerodynamic work distribution on blade surface

3.4 Results Comparisons

By comparing the experimental and numerical simulation results, the primary characteristics of flutter and NSV were obtained. To begin with, the frequency and phase lock were both observed during flutter and NSV with the first bending mode. The whole blades were tuned to the same frequency due to the separated flow in the cascade. Besides, the excitations were non-synchronized with the engine order due to the flow separation. Meanwhile, the frequency connection between the dynamic stress in the rotatory frame and the dynamic pressure in the stationary has proved that the two vibrations are flow-induced vibration. However, the flutter demonstrated a four nodal diameter forward wave vibration whereas NSV presented a 13 nodal diameter backward wave vibration. The lobed shape of blade tip vibration further proved the nodal vibration. Another distinction is that the aerodynamic damping for flutter was negative while for NSV was positive. Consequently, the blade stress would burst during flutter but the NSV offered stable stress level.

4. Conclusions

1) Using the multi-physical field measurement system, the basic characteristics of the fan blade flutter at 0.75 corrected speed and the compressor NSV at idle condition were obtained. Locked frequency and phase, nodal vibration form, non-integer engine order excitations were found to be the common features for flow-induced vibrations. The blade tip vibration showed lobed shape vibration in the optical fibre sensors.

2) The aerodynamic damping for the investigated flutter and NSV cases were -1.436E-3 and 5.067E4 respectively, indicating that the flutter would burst due to the negative aerodynamic damping. Correspondingly, experimental results showed that flutter stress soared rapidly to 187 MPa while NSV sustain at acceptable stress level reaching 150MPa.

3) The fundamental characteristic for flutter and NSV was that the link between the vibration

frequency and dynamic pressure characteristic frequency. Flutter was proved to be 4 nodal forward wave vibration while NSV was 13 nodal backward wave vibration.

5. Contact Author Email Address

Liu Yixiong: yixiong.liu5021@gmail.com

6. Copyright Statement

7. Acknowledgement

The authors would like to thank AECC Shenyang Engine Research Institute for the support and fund.

References

[1] Kielb R E., John W. Barter Jeffrey P.Thomas. Blade Excitation By Aerodynamic Instabilities- A Compressor Blade Study, *ASME Paper.* No.GT2003-38634, 2003.

[2] Zhizhong FU, Yangrong Wang,etc. Tip Clearance Effects on Aero-elastic Stability of Axial Compressor Blades[J]. *Journal of Engeering for Gas Turbine and Power*, 2015.

[3] Jeffers, II, J. D., Meece, Jr., C. E. F100 Stall Flutter Problem Review and Solution, *Journal of Aircraft*, 12(4), 350–357. 1975.

[4] El-Aini, Y. M., Capece, V. M. Stall Flutter Prediction Technique for Fan and Compressor Blades, *AIAA Paper* No. 95-2652, 1995.

[5] Marshall J. G, Imregum M. A.Review of aeroelasticity methods with emphasis on turbomachinery applications[J]. *Journal of Fluids and Structure*,1996,10:237-267, 1996.

[6] Bendiksen O O, Friedmann P P. The effect of bending-torsion coupling on fan and compressor blade flutter[J]. *ASME Journal of Engineering for Power*,1982,104:617-623, 1982.

[7] Fu ZH , Wang YR ,etc. Mistuning Effects on Aero-elastic Stability of Axial Compressor Rotor Blades[J]. *Journal of Engeering for Gas Turbine and Power.* October 2015,Vol. 137 102504-1-12, 2015.

[8] Hanamura, Y., Tanaka, H., Yamaguchi, K. A Simplified Method to Measure Unsteady Forces Acting on the Vibrating Blades in Cascade, Bull.JSME, 23(180), pp. 880–887,1980.

[9] Carta FO. Coupled blade-disk-shroud flutter instabilities in turbojet engine rotors. *ASME Journal of Engineering for Power*, 1967, 89: 419427, 1967.

[10] Bendiksen O. Aeroelastic problems in turbomachines.*AIAA-90-1157*. 1990.

[11] Snyder L E, Commerford G L. Supersonic Unstalled Flutter in Fan Rotors: Analytical and Experimental Results[J]. *Journal of Engineering for Gas Turbines and Power*, 1974, 96(4): 379-386, 1974.

[12] Erdos J I, Alzner E, McNally W. Numerical Solution of Periodic Transonic Flow through a Fan Stage[J]. *AIAA Journal*, 1977, 15(11): 1559-1568,1977.

[13]He L. An Euler Solution for Unsteady Flows Around Oscillating Blades[J]. *Journal of Turbomachinery*, 1990, 112(4): 714-722, 1990.

[14] He L, Denton J D. Three-Dimensional Time-Marching Inviscid and Viscous Solutions for Unsteady Flows Around Vibrating Blades[J]. *Journal of Turbomachinery*, 1994, 116(3): 469-476, 1994.

[15] Sanders A.J., Hassan K.K., Rabe D.C. Experimental and Numerical Study of Stall Flutter in a Transonic Low-Aspect Ratio Fan Blisk, Transactions of the ASME 2004,126(1):166-174,2004.

[16] Baumgartner M., Kamerier F., Hourmouziadis J.Non-Engine Order Blade Vibration in a High Pressure Compressor, *ISABE-Twelfth International Symposium on Airbreathing Engines*, Melbourne, Australia ,September 10-15,1995.

[17] Kameier, F.,Neise, W., 1995 I: Reduction of Tip Clearance Loss and Tip Clearance Noise in Axial-Flow Machines, *AGARD PEP 85th Meeting on Loss Mechanisms and Unsteady Flows in Turbomachines*, Derby, UK;8-12 May, 1995.

[18] Kameier, F., Neise, W., 1995 II: Rotating Blade Flow Instability as a Source of Noise in Axial Turbomachines, *Proc. 1st CEAS/AIAA Aeroacoustic Conference München*, June 12-15.

[19] Gill J., Capece V., Experimental investigation of flutter in a single stage Unshrouded Axial-Flow Fan, *42nd AIAA Aerospace Sciences Meeting and Exhibit.* 5 - 8 January 2004, Reno, Nevada, AIAA 2004-686, 2004.

[20] Tim R., David B., Gurnam S., Identification of the Stability Margin Between Safe Operation and the Onset of Blade Flutter, *Proceedings of ASME Turbo 2008*: Power for Land, Sea and Air. May 14-17,2007,Montreal ,Canada (GT2007-27462), 2008.

[21] Johann E., Muck B., Nipkau J. Experimental and Numerical Flutter Investigation of the 1st Stage Rotor in 4-Stage High Speed Compressor, *Proceedings of ASME Turbo 2008*: Power for Land, Sea and Air. June 9-13,2008,Berlin,Germany (GT2008-50698), 2008.

[22] Carta, F. O., St. Hilaire, A. O. Effect of Interblade Phase Angle and Incidence Angle on Cascade Pitching Stability, *ASME J. Eng. Power*,102, pp. 391–396, 1980.

[23] Buffum, D. H., Capece, V. R., King, A. J., El-Aini, Y. M. ExperimentalInvestigation of Unsteady Flows at Large Incidence Angles in a Linear Oscillating Cascade, *AIAA Paper* No. 96-2823,1996.

[24] Hardin, L. W., Carta, F. O., Verdon, J. M. Unsteady Aerodynamic Measurements on a Rotating Blade Row at Low Mach Number, *ASME Paper* No. 87-GT-221,1987.

[25] Huang, X.Q., He, L., Bell, D.L. Influence of Upstream Stator on Rotor Flutter Stability in a Low Pressure Steam Turbine Stage, *Proceeding of the IMechE Part A Jounal of Power and Energy*, Volume 220,NO.1, pp.25-35, 2006.

[26] Sun H, Yang L, Li HX Sensitive Flutter Parameters Analysis with Rescept to Flutter-Free Design of Compressor Blade, *APISAT2014*,2014 Asia-Pacific International Symposium on AeroSpace Technology, APISAT2014.

[27] Wu H, Yang M S, Wang D Y, et al. Construction and application of synchronized test system of multi-dynamic parameters [J]. *Acta Aeronautica et Astronautica Sinica*, 2014,35(2):391-399(in Chinese).

[28] LIU YX, LIU TY, WANG DY, et al. Numerical study of flutter prediction based on energy method and engevalue method[J]. *Aeroengine*，2014,40(6):43-46 (in Chinese).